*R*estoration of brain consciousness *ex vivo* after circulatory death in pigs

Guo ZY[1,2,3,†,*], Sun CJ[1,2,3,†], Xu GX[4,†], Yin MX[1,2,3,†], Zhu CH[1,2,3], Zheng DH[5], Zhang YX[1,2,3], Wang LH[1,2,3], Xie RX[1,2,3], Zhang ZH[1,2,3], Gao NX[1,2,3], Huang SZ[1,2,3], Yu P[6], He SJ[1,2,3], Zhao Q[1,2,3,*], He XS[1,2,3,*]

[1]Organ Transplant Center, The First Affiliated Hospital, Sun Yat-sen University, Guangzhou 510080, China

[2]Guangdong Provincial Key Laboratory of Organ Donation and Transplant Immunology, Guangzhou 510080, China

[3]Guangdong Provincial International Cooperation Base of Science and Technology, Guangzhou 510080, China

[4]Department of Neurosurgery, The First Affiliated Hospital, Sun Yat-sen University, Guangzhou 510080, China

[5]Intensive Care Unit, The First Affiliated Hospital, Sun Yat-sen University, Guangzhou 510080, China

[6]Center for Neurobiology, Zhongshan School of Medicine, Sun Yat-sen University Guangzhou 510080, China

[†]These four authors contribute equally to the article and should be considered as co-first authors

***Corresponding authors**

Guo ZY, Zhao Q and He XS, Organ Transplant Center, The First Affiliated Hospital, Sun Yat-sen University, No. 58 Zhongshan Er Road, Guangzhou 510080, China; Tel and fax.: 86-20-87306082; E-mail addresses: rockyucsf1981@126.com, zhaoqiang_china@sina.com & gdtrc@163.com

Author contributions

Guo ZY, Zhao Q and He XS designed the research; Guo ZY, Sun CJ, Huang SZ, Zheng DH, Xie RX and Zhao Q developed the surgical procedure. Guo ZY, Zhu CH, Wang LH, He SJ and

Zhang ZH performed the perfusion experiments and analyzed the data. Yu P, Zheng DH and Xu GX detected the MCA blood flow and EEG studies and analyzed the data. Sun CJ, Yin MX and Xu GX collected the tissue samples, analyzed and quantified the histological data. Guo ZY and Gao NX promoted the metabolomics and analyzed the data. Guo ZY and He XS wrote the manuscript and prepared figures. All author discussed and commented on the data.

Abstract

In clinical practice, a patient is declared dead after 30 minutes of unsuccessful resuscitation post-cardiac arrest, as the brain is considered irreversibly damaged within minutes after cardiac arrest. A recent report showed that cellular function of the brain can be restored hours post-mortem in pigs. However, whether consciousness can be regained *ex vivo* is unknown. Herein, we developed normothermic machine perfusion (NMP) technology for *ex vivo* brain resuscitation after circulatory death. We found that perfusion of the brain alone was able to preserve circulation, cytoarchitecture, metabolic activity and brainstem function, but failed to regain consciousness. With supports of a functioning liver, global electrocorticographic activity and consciousness were restored. Brain function could be maintained for at least 22 hours. The technology was able to resuscitate consciousness of the brain suffering 50-min normothermic ischemia. These findings demonstrate that liver-assisting brain NMP can restore and maintain consciousness *ex vivo* after a prolonged interval post-mortem.

Keywords: consciousness; normothermic machine perfusion; cardiac death; brain resuscitation; brain function.

1. Introduction

Human beings can be legally declared dead if they show irreversible loss of all brain function (brain death) or all circulatory function (circulatory death). Due to the advances in life support therapy such as extracorporeal membrane oxygenation (ECMO), a patient can survive without his own circulatory function[1]. On the other hand, there is a long-held assumption that mammalian brains are irreversibly damaged within a few minutes after cessation of blood supply[2-4]. Based on this assumption, circulatory death is usually declared after 30 minutes of unsuccessful resuscitation post-cardiac arrest[5], because the brain is considered "dead" even the circulation can be restored by artificial techniques at this circumstance. In controlled donors after circulatory death, the patient is declared dead 2-5 minutes after their hearts stop beating and organ donation proceeds[6]. Indeed, a systemic analysis with inclusion of 493 donors showed that under strict observance of the 5-min interval, return of spontaneous cerebral and cardiac activity following asystole has not occurred to date[7].

However, emerging evidence challenges this assumption. In the cats and macaques, the neuronal, electrophysiological and metabolic function of the brain can be regained after 60-min global ischemia[8-11]. In the pigs, the brains can tolerate 30-min global ischemia under pressure-controlled reperfusion[12]. However, these studies used a heart-beating model, which is very different from the clinical scenarios of cardiac arrest. Besides, studies have shown that the cellular and mitochondrial functions of human brain tissue specimens can be well-preserved hours after death[13-15]. Most recently, Zvonimir *et al* reported successful restoration of circulation and cellular function in isolated pig brains four hours post-mortem by using a BrainEx system to re-establish their oxygen supply[16]. However, coordinated electrical pattern or consciousness has never been recorded in this system. Therefore, we should not consider it as successful recovery of brain function post-mortem and convincing evidence which can challenge the current diagnostic criteria of death is still lacking.

The BrainEx system actually used *ex vivo* normothermic machine perfusion (NMP) technology, which provides normothermic oxygen supply to the organs. NMP is not a new concept. Indeed, in 1960s, researchers tried to use NMP to test whether the brain function can be maintained *ex vivo*[17]. The study demonstrated that the metabolic and electrophysiological activity of the brains can be restored but deteriorated quickly (2-3 hours) even after very short

ischemia time. This might be explained by the under-developed NMP technology at that time. Recent reports showed that *ex vivo* NMP is able to resuscitate function of human hearts, lungs, livers and kidneys after circulatory death[18-21]. However, it is still unknown whether NMP can also resuscitate the brain function.

Notably, the Yale group did not aim to restore the brain consciousness[16]. Besides, the technological characteristics might explain why global electrophysiological activity could not be regained in their model. Firstly, the brain may be probably not able to tolerate the long normothermic ischemia time (60 min) and total ischemia time (240 min). Secondly, the brain is highly sensitive to the changes of environment. The BrainEx system may be not able to provide suitable conditions, such as metabolic environment for the restoration of brain function. Finally, as claimed in their paper, various antagonists were added in the perfusate to prevent possible electrophysiological recovery.

In this study, we designed to test whether consciousness can be restored *ex vivo* after circulatory death and what is the ischemic interval limit after which it can be regained. The *ex vivo* brain NMP technology contains surgical techniques to isolate the brain, suitable perfusate, machine perfusion device and brain function assessment techniques. We firstly perfused the brain alone immediately after circulatory death and found that only brainstem function were restored. Then a liver was added into the perfusion circuit to provide metabolic supports for brain resuscitation, which successfully help restore and maintain consciousness as assessed by behavior monitoring, consciousness scoring and electrophysiological recording. Subsequently, the normothermic ischemia time was carefully prolonged and the brain function could be recovered after 50 minutes post-cardiac arrest. Finally, the perfusate metabome analysis, and RNA sequencing analysis and proteomics analysis of brain tissue were conducted to dissect the possible molecular mechanisms. The results in this study demonstrated evidence that brain consciousness can be restored and maintained *ex vivo* after circulatory death.

2. Methods

2.1 The placement of electrodes

The reference electrodes were placed on A1, A2 and Cz, and the ground electrode was placed on Fz. The electrodes were placed according to the international 10-20 system, the

electrode names begin with one or two letters indicating the general brain region or lobes where the electrode was placed (Fp, fronto-polar; F, frontal; C, central; P, parietal; O, occipital; T, temporal). Each electrode name ended with a number or letter indicating the distance to the midline. Odd numbers were used in the left hemisphere, even numbered in the right hemisphere. Larger numbers indicated greater distances from the midline, while electrodes placed at the midline were labeled with a "z" for zero. Cz was placed over midline central brain regions and Fz was placed over midline frontal brain regions. A1 and A2 electrodes were placed on the left and right ears, respectively.

2.2 Sample preparation, UHPLC separation and raw data processing for metabolomics analysis

100 μL of sample was transferred to an EP tube, and 400 μL extract solution (acetonitrile: methanol = 1: 1) containing internal standard (L-2-Chlorophenylalanine, 2 μg/mL) was added. After 30 s vortexed, the samples were sonicated for 5 min in ice-water bath. Then the samples were incubated at -40°C for 1 h and centrifuged at 10000 rpm for 15 min at 4°C. 425 μL of supernatant was transferred to a fresh tube and dried in a vacuum concentrator at 37°C. Then, the dried samples were reconstituted in 200 μL of 50% acetonitrile by sonication on ice for 10 min. The constitution was then centrifuged at 13000 rpm for 15 min at 4°C, and 75 μL of supernatant was transferred to a fresh glass vial for LC/MS analysis. The quality control (QC) sample was prepared by mixing an equal aliquot of the supernatants from all of the samples.

The UHPLC separation was carried out using an Agilent 1290 Infinity series UHPLC System (Agilent Technologies), equipped with a UPLC BEH Amide column (2.1 * 100 mm * 1.7 μm, Waters). The mobile phase consisted of 25 mmol/L ammonium acetate and 25 mmol/L ammonia hydroxide in water (pH = 9.75) (A) and acetonitrile (B). The elution gradient was set as follows: 0~1.0 min, 95% B; 1.0~14.0 min, 95%~65% B; 14.0~16.0 min, 65%~40% B; 16.0~18.0 min, 40% B; 18.0~18.1 min, 40%~95% B; 18.1~23.0 min, 95% B. The flow rate was 0.5 mL/min. The column temperature was 25°C. The auto-sampler temperature was 4°C, and the injection volume was 2 μL (pos) or 2 μL (neg), respectively. An Agilent 6495 triple quadrupole mass spectrometer (Agilent Technologies) was applied for assay development in a multi-reaction monitoring (MRM) mode. Capillary voltage = +3000/-2500 V, gas (N_2) temperature = 170°C, gas (N_2) flow = 16 L/min, sheath gas (N_2) temperature = 350°C, sheath gas flow = 12 L/min, nebulizer = 40 psi, Fragmentor = 380

V.

The format for MRM raw data (.d files from Agilent data acquisition software MassHunter B.06.00) were first converted to files in mzML format using the "msconvert" program from ProteoWizard (version 3.0.6526). Then the mzML files were converted into text format files using the "mscat" program incorporated in ProteoWizard (version 3.0.6526) so that the data can be loaded into R and processed by MRMAnalyzer. The generated text format files contain four columns: transition index, Q1 and Q3 specifications of MRM transitions, retention time and intensity, respectively. The MRM data processing using the MRMAnalyzer includes five steps: "pseudo" accurate m/z transformation, peak detection and alignment, metabolite identification, quality control check and statistical analysis[22].

2.3 Surgical preparation of the porcine heads and livers

A total of 20 Tibet mini-pigs (purchased from Southern Medical University, Guangzhou, China, 30-50 kg) were used during development of the brain NMP technology. The study protocol was reviewed and approved by the Animal Ethical Committee of The First Affiliated Hospital of Sun Yat-sen University. Circulatory death was induced by exsanguination and ventricular injection of 1g potassium chloride. To mimic clinical organ donation after circulatory death, a 5-min no-tough time was waited before the head (and liver) was harvested. After the technology was optimized in the preliminary experiments, independent 27 brains were perfused, and 5 brains harvested immediately after circulatory death were used as controls in pathological assessment, data from which are presented herein.

In the BAI group, after anesthesia, the skin, connective tissues and musculature around the connection between C7 and T1 vertebra were cut with a high-frequency electric knife. The bilateral common carotid arteries and veins were well-dissected and the vertebral arteries from subclavien arteries were ligated. Then thoracotomy was performed to expose the roots of common carotid artery trunk and jugular vein stem. Then, 62500 U heparin was intravenously injected. Exsanguination (800-1000 mL whole blood) from the abdominal aorta was conducted and followed by ventricular injection of 1g potassium chloride. At 5 minutes after cardiac arrest, the common carotid artery trunk and jugular vein stem were divided. The esophagus, trachea and spinal cord were disconnected. The head was harvested and immediately connected to the brain NMP system through the common carotid artery trunk. For the liver-assisting brain NMP

groups, the liver with the abdominal aorta (including celiac artery) and portal vein were well-dissected before exsanguination.

2.4 *Ex vivo* brain NMP technology

Our *ex vivo* brain NMP system consists of an arterial pump unit, a venous pump unit, an oxygenation unit, a filtration unit, a thermo unit and a control unit (Figure. 1A). The arterial pump unit uses a magnetic rotary pump to supply a pulsatile (60 beat per minute) whole-blood containing perfusate, with an adjustable perfusion pressure range of 0-110 mmHg and perfusion flow range of 0-1000 mL/min. The adjustable perfusion pressure range of the venous pump unit is 0-12 mmHg, with a perfusion flow of 0-2500 mL/min.

In the BAI group, a 16 Fr arterial cannula was inserted into the common carotid artery trunk to perfuse the brain. In the liver-assisting NMP groups, the abdominal aorta (with the celiac artery) was connected to the common carotid artery trunk, and the 16 Fr arterial cannula was inserted into the abdominal aorta to simultaneously perfuse the liver and brain. Meanwhile, a straight 24Fr cannula was inserted to the portal vein to perfuse the liver. The artery pressure range was maintained at 90-100 mmHg to keep the left MCA flow close to the preoperative value.

2.5 Measurement of global cerebral metabolism

Hourly venous perfusate samples were collected from the jugular vein outflow of the brain during NMP. Arterial perfusate samples were collected from the common trunk carotid arterial inlet line to the brain every 20 minutes during the first three hours of perfusion, and then every half hour for the following three hours. One hundred microlitres of each sample was immediately analysed using the i-STAT®1 blood analyser system (Abbott; Flextronics, Singapore) with CG4+ and EC8+ test cartridges. Similarly, the arteriovenous gradients in glucose (GLU), lactate (Lac), PH, partial pressure of carbon dioxide and oxygen (PCO2, PO2) were calculated.

2.6 PET-CT scan

The PET-CT examination was performed on a Philips Gemini-GXL-PET-CT (Philips Healthcare, Netherlands). The perfusate glucose level prior to injection was <10 mmol/L. A standard injection of 4 mci 2-Deoxy-2-[^{18}F]fluoro-D-glucose ([^{18}F]FDG) was administered, followed by a 30-minute uptake period. The PET protocol used a 10-minute single bed

acquisition with the head positioned in an appropriate head restraint. Image reconstruction parameters were as follows: 120 kV, 250 mAs and 3.75-4 mm PET slice thickness in 144 × 144 matrix.

2.7 Global electrophysiological monitoring of the brains

After sedation but before tracheal intubation, the initial global EEG of pig brains was recorded. During *ex vivo* NMP, the global EEG of isolated pig heads was recorded continuously throughout NMP. Real-time detection and assessment of global EEG from scalp were performed by qEEG analysis system (NicoletOne software version 5.94, Natus Medical Inc, San Carlos, CA, USA). The spectral entropy of qEEG was utilized to assess the conscious states of the isolated pig heads, especially for the awake state. Global EEG was recorded from 12 silver disc electrodes (Fp1, Fp2, C3, C4, T3, T4, O1, O2, Fz, Cz, A1 and A2). The placement of electrodes is provided in the Supporting Information.

2.8 Transcranial doppler (TCD) cerebral blood flow chart

After sedation but before tracheal intubation, the initial cerebral blood flow signal charts of the pigs were measured. During *ex vivo* NMP, the cerebral blood flow signal chart measurement of isolated pig head was performed every hour. The signal chart of cerebral blood flow was acquired from the left MCA through the ocular windows (depth range 4-4.5cm) with 1.6 MHz probe by TCD (EMS-9PB, Delica, Shenzhen, China). The peak blood flow value of TCD waveform was used to evaluate the cerebral blood flow.

2.9 Assessment of conscious states by Full Outline of UnResponsiveness (FOUR) score and daily behavior monitoring

The conscious state of isolated pig heads during *ex vivo* NMP was assessed by the FOUR score. The FOUR score is a coma assessment scale, which consists of four components (eye response, motor response, brainstem reflexes, and respiration) and each component has a maximal score of 4[23]. The score of these four components was recorded every hour throughout NMP. All the procedures of scoring were recorded by videos. We also assessed the foraging, drinking water and responses to the pig's voice. In addition, these properties of consciousness can be explained at the neural, behavioral, and phenomenal levels. The assessment of daily behaviors was carried out hourly and recorded by videos. The cerebral cortex response of isolated pig heads was evaluated by performing intensive light and sound stimulation. The

responses to these stimuli, such as closure of eyelids and ear movement, were recorded by videos. The EEG reactivity referring to any change in frequency or amplitude due to light and sound stimulation was recorded by qEEG analysis system.

2.10 Tissue processing and histology

Tissue section preparation. Following the endpoint of each experiment, the whole brain was obtained from the head and handled as follows. The tissues were dissected into 7-mm-thick blocks and fixed for 4 days in 4% paraformaldehyde at 4°C. Tissues were trimmed into 5-mm-thick slabs and placed in dehydration boxes. Tissues was then dropped stepwise into 75% alcohol for 3.5 h, 85% alcohol for 2 h, 90% alcohol for 2 h, 95% alcohol for 1 h, and 100% alcohol for 40 min. Samples were sequentially cleared with the mixture contained 50% alcohol and 50% dimethyl benzene for 5 min, dimethyl benzene I for 5 min, dimethyl benzene II for 5 min. Tissues were immersed in paraffin I for 1 h, paraffin II for 1 h, paraffin III for 1 h. Eventually, blocks were embedded in melted wax, cooled into a wax block at -20° freezing table, and sectioned into 3-5μm section using the pathological slicer (Shanghai Leica Instrument, RM2016). Slices were mounted on anti-off slide.

HE staining. Sections were serially dewaxed in dimethyl benzene I for 20 min, dimethyl benzene II for 20 min, 100% alcohol I for 5 min, 100% alcohol II for 5 min, 75% alcohol for 5 min, and washed with ddH_2O for 3 min. Tissue sections were counterstained with hematoxylin for 4 min, flushed with water; differentiated by hydrochloric acid aqueous solution for 10 s, rinsed with water; and dyed by aqueous ammonia (Sinopharm Chemical Reagent Co., Ltd, 10002118, China), flushed with water. Section were serially dehydrationed in 75% alcohol, 85% alcohol and 100% alcohol, and embedded in eosin solution for 5 min. Samples were serially dehydrated in 100% alcohol I, 100% alcohol II, 100% alcohol III, n-butyl alcohol, dimethyl benzene I, and dimethyl benzene II for 5 min in each step. Finally, slices were sealed by neutral gum.

TUNEL staining. Sections were serially dewaxed in dimethyl benzene I, dimethyl benzene II, and dimethyl benzene III for 15 min in each step; washed by 100% alcohol I, 100% alcohol II, 85% alcohol, and 75% alcohol for 5 min in each step; rehydrated in ddH_2O for 5 min. Section was encircled by a circle drew by immunohistochemical pen to prevent liquid from flowing away. The tissue was covered with proteinase K solution (Servicebio, G1205,

China) in the circle, incubated for 25 min in a 37°C incubator and rinsed with PBS (pH=7.4) (3 × 5 min). After incubated in the cell membrane breaking solution (Servicebio, G1204, China) for 20 min at room temperature, sections were washed thrice. Appropriate reagent A (TdT) and reagent B (dUTP) in the TUNEL kit (Roche, 11684817910, Switzerland) were mixed 1:9, and added into slices to incubate for 2 hours in a 37°C incubator. Tissues were rinsed thrice and dyed by DAPI staining solution (Servicebio, G1012, China) at room temperature in dark for 10 min. Samples were washed thrice and sealed with an anti-fluorescence quenching agent (Servicebio, G1401, China)

Nissl staining. Sections were serially dewaxed as the step of HE staining. Tissue was stained with 1% toluidine blue (Servicebio, G1032, China) for 5 min. Sections were quickly rinsed in ddH_2O and then differentiated in 1% glacial acetic acid. The degree of differentiation was controlled under the microscope, and the slices were roasted. Slides were cleared in dimethyl benzene for 5 min, dried slightly, and sealed by neutral gum.

Immunohistochemistry (IHC). Section were serially dewaxed as the step of TUNEL staining. After rehydrating, tissue sections were suffered to antigen retrieval using retrieval fluid (pH=9.0) (Servicebio, G1203, China) and washed in PBS (pH=7.4) (3 × 5 min). Endogenous peroxidases of tissues were quenched with 3% H_2O_2 for 25 min at room temperature, and protected from light. Slides were blocked in 3% bovine serum albumin (BSA) (Servicebio, G5001, China) for 30 min before incubation with primary antibody overnight at 4°C. The primary antibody included: HIF-1α (Hypoxia-inducible factor 1-alpha; mouse anti-HIF-1 alpha; 1:100; Abcam; ab16066); Hsp70 (Heat shock 70 kDa protein; mouse anti-Hsp70; 1:200; Abcam; ab47454); and NRF2 (Nuclear factor, erythroid 2 like 2; rabbit anti-NRF2/NFE2L2; 1:200; Proteintech; 16396-1-AP). Unconjugated primary antibodies were rinsed with PBS (pH=7.4) (3 × 5 min). HRP-conjugated secondary antibodies corresponding species of the primary antibody were dropped on slides to cover the tissue and incubated for 50 min at room temperature. Unconjugated secondary antibodies were washed with PBS (pH=7.4) (3 × 5 min). Freshly prepared DAB coloring solution (Servicebio, G1211, China) was dropped to cover the sample. Action time was depended on color rendering under the microscope. Development of color reaction was terminated by water flush. The positive color was brownish-yellow.

Tissue sections were counterstained with hematoxylin for 3 min, flushed with water;

differentiated by hematoxylin differentiation solution for 10 s, rinsed with water; and dyed by the hematoxylin blue liquid (Servicebio, G1340, China), flushed with water. Nuclei were dyed blue. Section were serially dehydrated in 75% alcohol, 85% alcohol, 100% alcohol, dimethyl benzene I, and dimethyl benzene II for 5 min in each step. Finally, slices were sealed by neutral gum.

Immunofluorescence (IF). Sections were serially dewaxed as the step of HE staining. Tissues were suffered to antigen retrieval using retrieval fluid (pH=8.0) (Servicebio, G1202, China) and washed in PBS (pH=7.4) (3 × 5 min). Samples were incubated with autofluorescence quencher agent for 5 min and washed with running water for 10 min. Slides were blocked in 3% BSA for 30 min before incubation with primary antibody overnight at 4°C. The primary antibody included: IBA1 (Ionized calcium binding adapter molecule 1; goat anti-Iba1; 1:100; Abcam; ab5076); GFAP (Glial fibrillary acidic protein; mouse anti-GFAP; 1:100; Sigma; G3893); GAD1 (Glutamate decarboxylase 1; goat anti- GAD1; 1:100; R&D systems; AF2086); and NRGN (Neurogranin; sheep anti-NRGN; 1:100; R&D systems; AF7947). The nucleus were dyed with DAPI. Tissues were washed thrice and sealed with an anti-fluorescence quenching agent.

Microscopy and image processing. Images of HE, TUNEL and Nissl staining were viewed by an upright microscope (NIKON, ECLIPSE CI, Japan) equipped with a imaging system (NIKON DS-U3). IHC and IF were visualized using the fluorescence microscope (CIC, XSP-C204, China) and a Case Viewer (3D HISTECH, Pannoramic MIDI, Hungary), respectively.

Histological data analysis and quantification. Images (using the 10× or 20× objectives as described previously) of samples dyed for TUNEL, Nissl, IHC or marker protein (GAD1, NRGN, GFAP and IBA1**)** were standardized to equivalent image area, randomized, and summarized by a blinded participant for the interested fields. For all images, cells were retained if exceeding the lowest intensity level, not presenting vacuoles larger than nucleus, or not indicating mechanical injury of cells. Randomized observer-blinded trial was used to process the figures as described earlier. Interested objects were counted using the tally function in ImageJ software (NIH).

2.11 Metabolomics analysis of the perfusate during *ex vivo* brain NMP.

Perfusate samples from the arterial perfusion line at 2 and 3 hours after NMP were collected in the BAI and LABI groups. Triple samples were retained at each time point. The detailed protocol of sample preparation, UHPLC separation and raw data processing is provided in the Supporting Information. The data were analyzed by means of Statistical Analysis System (SAS Institute Inc., Version 9.0). Statistical significance was declared at $P < 0.05$. The resultant three-dimensional data involving the peak number, sample name, and normalized peak area were fed to a SIMCA software package (v14.1; Sartorius Stedim Data Analytics AB; Umea, Sweden) for principal component analysis (PCA) and orthogonal projections to latent structures–discriminate analysis (OPLS–DA). PCA showed the distribution of original data. To obtain an enhanced level of group separation and obtain an increased understanding of variables responsible for classification, supervised OPLS–DA was applied. This permutation test was conducted to validate the mode. On the basis of OPLS–DA, a loading plot was constructed showing the contribution of variables to differences between the two groups. To refine this analysis, the first principal component of variable importance in the projection (VIP) was obtained. If $P < 0.05$ and $VIP > 1$, then the variable was defined as a significantly differential metabolite between the groups. Using the Kyoto Encyclopedia of Genes and Genomes (KEGG, http://www.genome.jp/kegg), metabolic pathways mapped by every differential metabolite were acquired.

2.12 RNA sequencing analysis

In brief, isolation of total RNA and RNC-RNA was used by TRIzol Reagent, according to the manufacturer's instructions. Total RNA was performed for subsequent RNA-seq. The polyA+ mRNA was selected from the total RNA samples by RNA Purification Beads (Vazyme). The cDNA library products were generated using VAHTS mRNA-seq V2 Library Prep Kit for Illumina and sequenced using the Illumina HiSeq X Ten. Library construction and sequencing were performed at Shenzhen Chi-Biotech Corporation. High-quality reads were kept for the sequence analysis by the Illumina quality filters. The mRNA abundance was normalized using rpkM. Genes with > 10 mapped reads were considered as quantified genes. The edgeR package method was adopted to analyze the differential expression genes.

2.13 Proteomics analysis

After dithiothreitol (DTT) added to reduced disulfide bond and iodoacetamide added (IAA)

to alkylated, ice acetone was added to samples for proteins precipitation 5h at -20 ℃. 1000g centrifugation at 4 ℃ collected the protein pellets and wash two times with ice acetone. Then, pellets was dissolved with 25 μL trypsin (Promega, Madison, WI) solution (in 50 mM ammonium bicarbonate，20 ng/ μL) with strongly vortex and then incubated at 37 ℃ overnight. Trypsin-digestion peptides desalted with Pierce C18 spin tips (Thermo Scientific, MA, USA) under the guidance of its specification before LC-MS/MS analysis.

The peptides were resuspended with 20 μL solvent A (solvent A: water with 0.1% formic acid) and analyzed by on-line nanospray LC-MS/MS on an Orbitrap Fusion coupled to an EASY-nano-LC system (Thermo Scientific, MA, USA). The analysis was performed on each fraction, with MS1 mass resolution of 350-1550 and MS/MS resolution of 30 K under HCD mode.

All MS/MS raw data were analyzed using Maxquant 1.5.2.8 with the LFQ method. Andromed was set up to search "Swissprot pig protein database. fasta" (Download in 12/2019, 104050 entries) assuming the digestion enzyme trypsin. Andromed was searched with a fragment ion mass tolerance of 0.020 Da, a parent ion tolerance of 10.0 PPM and max miss cleavage of 2. Carbamidomethyl of cysteine was specified in Sequest as fixed modifications. Oxidation of methionine and acetyl of the n-terminus were specified in Sequest as variable modifications. Protein identifications was controlled by both peptides and proteins FDR < 0.01 and unique peptides ≥ 1.

2.14 Measurement of serum S100-β level

The perfusate samples from arterial perfusion line were collected and shaken. 80 μL samples were dropped onto the chip of S100-β Rapid Test Kit (Immunochromatography) (Wuhan Easy Diagnosis Biomedicine, China). The chip was incubated 15 min and tested in an immunoassay analyzer (Wuhan Easy Diagnosis Biomedicine Co., QMT8000, China).

2.15 Statistics and reproducibility

All data are presented as the mean ± s.e.m. Data analysis was conducted using paired and unpaired t-tests, repeated ANOVAs. The number of brains per control group and experimental group, as well as appropriate statistical analyses, are specified in each figure legend. In Figure. 2A, the two-tailed paired t-tests were used to compared the MCA blood flow between NMP duration and pre-operation. In Figure.2, D and F, the unpaired t-tests were used to compared

the apoptotic cells in Cortex and Hippocampus between normal group and the other group, or between BAI group and the other group. In Figure. 2F, the two-tailed paired t-tests were used to compared the blood gas parameters between arterial and venous during NMP. In Figure. 3, C to E, the unpaired t-tests were used to compared the Four score, MCA blood flow, and S100-β between BAI group and LABI group during NMP. In Figure.4, B and C, the unpaired t-tests were used to compared the Neuronal cell density cells in CA1 field (B) and Dentate gyrus field (C) between normal group and the other group, or between BAI group and the other group. In Figure.4, E and F, the unpaired t-tests were used to compared the GAD1 staining cells (E) and NRGN staining cells (F) in Cortex field between normal group and the other group, or between BAI group and the other group. In Figure.4, H and I, the unpaired t-tests were used to compared the immunofluorescent stains for microglia (IBA1) in CA1 field (H) and Dentate gyrus field (I) between normal group and the other group, or between BAI group and the other group. In Figure.4, K and L, the unpaired t-tests were used to compared the immunofluorescent stains for astrocytes (GFAP) in CA1 field (H) and Dentate gyrus field (I) between normal group and the other group, or between BAI group and the other group. In Figure.4N, the unpaired t-tests were used to compared metabolites between BAI and LABI group.

All statistical analyses by SPSS 20.0 (SPSS Inc, Chicago, Illinois, USA) and data plotting were conducted using GraphPad 8 (GraphPad Software, Inc.). All figures were assembled using Adobe Illustrator CC (Adobe System, Inc.). $P<0.05$ was considered to indicate a significant difference from the control.

3. Results

3.1 Overview of technology of *ex vivo* brain NMP

Our *ex vivo* brain NMP system consists of an arterial pump unit, a venous pump unit, an oxygenation unit, a filtration unit, a thermo unit and a control unit (Figure. 1a). The flowing perfusate passes through the oxygenation unit and is heated by the heater, then passes through the filtration unit and perfuses the brain/liver. The oxygenation unit maintains the PO_2 and PCO_2 of the perfusate with expected ranges by adjusting the air flow to ensure metabolic needs for the brains. The filtration unit filters out tiny blood clots and impurities, and the thermo unit maintains the temperature of the perfusate at 38°C. The operating interface of the control unit monitors and adjusts the perfusion pressure and temperature.

The system circulated a whole blood-based perfusate (Table S1) with a pulsatile artery line and non-pulsatile portal vein line. The arterial perfusion pressure gradually increased from 60 mmHg to 90-100 mmHg in 10 minutes to achieve a middle cerebral artery (MCA) flow close to the preoperative value. The portal vein perfusion pressure was set at 5-12 mmHg to maintain a flow higher than 500 mL/min.

The brains were re-perfused *ex vivo* immediately or after various warm ischemia times (WIT) with or without combined perfusion of a liver. When the livers were used, they were re-perfused *ex vivo* as soon as they were harvested to ensure their viability (Figure. 1B). In this study, we designed six experimental groups: brain alone immediately NMP group (BAI group, n = 5); liver-assisting brain immediately NMP group (LABI group, n = 5); liver-assisting brain 30 min-WIT NMP group (LABWI-30 group, n = 5); liver-assisting brain 50 min-WIT NMP group (LABWI-50 group, n = 5); liver-assisting brain 60 min-WIT NMP group (LABWI-60 group, n = 4); liver-assisting brain 240 min-WIT NMP group (LABWI-240 group, n = 3).

During NMP, electroencephalogram (EEG) was monitored to detect the electrical activity of the brains. Transcranial Doppler (TCD) was used to monitor the MCA flow. The blood gas analysis of the perfusate was performed to guide adjustment of gas supply and perfusate components. Intracranial pressure was measured by a pressure tube that passed through the cervical spinal stump into the cerebellar medullary cistern. A shot of 50 mL mannitol was used when the intracranial pressure exceeded 80 mmH_2O. A dose of 0.5 mg nimodipine was used when the MCA flow was 10 cm/s lower than the preoperative value. A dose of 50 mg Tramadol

Hydrochloride Injection was added in the perfusate to reduce pain in case it was presented.

3.2 Preservation of tissue integrity, metabolic activity and brain stem function after brain-alone NMP

Firstly, we tested whether NMP of brain alone immediately after circulatory death (BAI group) was able to resuscitate consciousness. Due to the 5-min no-touch time and NMP preparation, the brains suffered 10.1 ± 1.8 min WIT in this group (Figure. 1B). The TCD detection showed that the pre-operative flow of the left MCA was 38.8 ± 9.6 cm/s. The flow was close to the pre-operative level at the beginning of NMP, but started to decline after 6-hour perfusion even when nimodipine was used to dilate the vessels (Figure. 2A). The general structure of the whole brains was preserved (Figure. S1). The hematoxylin and eosin (HE) staining demonstrated the tissue integrity was restored, although obvious ischemia-reperfusion injuries in the cortex, thalamus, hippocampus, cerebellum and brainstem were observed when compared to the healthy controls (Figure. 2B). The terminal deoxynucleotidyl transferase-mediated biotinylated UTP nick end labeling (TUNEL) showed 11.2% and 6.0% apoptotic cells in the cortex and hippocampus, respectively (Figure. 2, C to E). These data demonstrated that brain circulation and tissue integrity were preserved during *ex vivo* NMP.

We then investigated whether restored blood supply to the brains could re-activate the global metabolic activity. The arterial and venous samples were compared throughout the course of experiments. Consistent with the previous studies[16,24], the arteriovenous gradients demonstrated consistent consumption of glucose and oxygen during NMP, with concurrent production of CO_2 and a physiological drop in pH values (Figure. 2F). Recently, a study reported that both the brains and muscles are major organs releasing lactate[25], which might explain the increasing lactate levels during perfusion. Since the head contains tissues other than the brain, the arteriovenous gradients reflected the global metabolic activity of the whole head. To evaluate the metabolic activity of the brain, a positron emission computed tomography (PET-CT) scan was done and showed that the cerebrum (standard uptake value: 0.09), cerebellum (standard uptake value: 0.08) and brainstem (standard uptake value: 0.08) were under active glucose metabolism (Figure. 2G). These results confirmed that metabolic activity of the brain was regained during *ex vivo* NMP.

A previous study showed complete recovery of pig brain function after global ischemia[26],

during which the brain was resuscitated *in vivo* with heart beating (the full function of organs other than the brain was preserved). In the current model, some brainstem reflexes, such as corneal reflex and pupillary light reflex, were presented during *ex vivo* NMP. Besides, the pig heads showed spontaneous respiration and its frequency increased along with the increased pCO_2 level in the perfusate (video S1). However, the EEG monitoring did not document any kind of organized global electrical activity in this group (Figure. 2H), although they looked like awake. Obvious edema of the re-perfused brains (Figure. S1) and increased arterial resistance (Figure. S2C) occurred, which are in consistence with a previous study in monkeys[17]. These findings suggest that *ex vivo* NMP of the brain alone is able to restore brainstem function, but it fails to restore consciousness.

3.3 *Ex vivo* restoration of consciousness by addition of a liver in the NMP circuit

Hepatic encephalopathy or even hepatic coma is a common complication in patients suffering end-stage liver disease[27]. We hypothesized that global electric activity could not be restored *ex vivo* without the supports of a functioning liver. Therefore, a liver from the same pig was perfused along with the head in the system (LABI group). Because of the additional procedures, the WIT of the brains in this group (14.2 ± 0.7 min) was longer than those in the BAI group (10.1 ± 1.8 min) (P=0.067). The livers continued to produce bile during perfusion, indicating that they were functioning[28]. Under this circumstance, the EEG monitoring recorded frequent α waves and β waves (Figure. 3A), both of which represent the conscious activity of the brains[29,30]. Importantly, the *ex vivo* perfused heads presented with activities associated with high-order brain functions such as eyeball tracking, foraging and response to recorded pig voice (video S2). The Full Outline of UnResponsiveness (FOUR) score, which is used to assess the conscious state [23], was much higher in the LABI versus BAI group (3h-NMP: 8.2±0.7 versus 4.2 ± 0.2, P<0.001; 5h-NMP: 8.8 ± 0.4 versus 4.8 ± 1.7, P =0.0462) (Figure. 3C). The maximum FOUR score achieved 13 in the LABI group (Table S2), suggesting an almost conscious wake status of the *ex vivo* perfused brain. During the preliminary stage of establishing this system, the arousal (i.e. cycles of eye-opening and closing) and awareness of one isolated pig head, were maintained for 22 hours. The perfusion was stopped because the perfusionist was too tired to continue. Collectively, these data showed that consciousness can be restored *ex vivo* by combined brain and liver NMP.

3.4 Regained brain function 50 minutes after cardiac arrest

The previous *in vivo* study showed that the pig brain can tolerate 30-min global ischemia[26], and a very recent *ex vivo* study reported that cellular function can be restored after 4-hour complete ischemia (1-hour warm ischemia plus 3-hour cold ischemia) with no sign of consciousness recorded[16]. To test the longest normothermia ischemia interval after which consciousness can be restored *ex vivo* in pigs, the brain WIT was extended to 30 minutes (LABWI-30), 50 minutes (LABWI-50), 60 minutes (LABWI-60), and 240 minutes (LABWI-240) in the current study. The brain consciousness could be retained in three out of five pigs after 2-3 hours of *ex vivo* NMP, as evidenced by EEG records (Figure. 3A), FOUR scores (Figure. 3A) and daily behaviors (video S3) in the LABWI-30 group. When the brains suffered 50-min WIT, consciousness was documented in one brain, although four of the five brains presented with brainstem function. In the case with consciousness, the eyelids were closed after stimulation by intensive light and the ears moved in response to intensive sound (video S4). The EEG reactivity referring to these stimuli in frequency and amplitude was recorded by quantitative EEG (qEEG) analysis system (Figure. 3B). In contrast, neither organized electrical activity nor brainstem reflex showed up in the brains suffering 60-min or 240-min WIT (Figure. 3A, Table S2). These results suggest that under proper conditions, brain function can be restored after unexpected long interval post-cardiac arrest.

3.5 Improved circulation and reduced neuronal injuries after liver-assisting versus brain alone NMP

It is of great importance to understand the roles of a functioning liver in *ex vivo* restoration of consciousness. Addition of the liver increased the MCA flow under similar arterial perfusion pressure (Figure. 3D), and substantially declined the perfusate level of S100-β (LABI versus BAI) (Figure. 3E), which is a biomarker of neural injury[31]. Interestingly, the S100-β level did not increase along with the prolonged WIT, which might be explained by the inhibition of protein synthesis. We subsequently assessed whether there were anatomical reflections in the cytoarchitectural integrity of brain regions which are highly susceptible to anoxia and ischemia, such as the neocortex, hippocampus, and cerebellum[32,33]. The HE staining demonstrated obvious pathological changes of cell shrinkage, nucleus pyknosis or perinuclear space expansion in cortical, hippocampal and cerebellar cells in the BAI group (Figure. 2B). In

contrast, pyramidal neurons had plump cell bodies with large centrically located nuclei and exuberant nerve fibers in the LABI group. The cytoarchitectures of the cortex, thalamus, hippocampus, cerebellum and brainstem in the LABI and LABWI-30 groups were comparable to those in the normal controls (Figure. S5). Besides, no significant increase of apoptotic cells in the hippocampus was documented in these two groups (Figure. 2, C to E). As the WIT prolonged, tissues of the cortex, hippocampus, cerebellum, brainstem and thalamus became looser with more severe vacuolation and cell shrinkage, deepened nuclear pyknosis, increased apoptotic and necrotic cells (Figure. 2, C to E; and Figure. S5). Interestingly, the cytoarchitecture was well-preserved in the LABWI-50 brain with consciousness (Figure. S6).

We further assessed the neuronal viability by Nissl staining. The results showed comparable density of live neurons in both CA1 field and dentate gyrus between the Normal and LABI/LABWI-30 groups. In contrast, there was a decreased density of live neurons in the CA1 field in the BAI group (Figure. 4, A to C). Immunofluorescent analysis for the inhibitory neuronal marker glutamate decarboxylase 1 (GAD1) revealed preserved cell density in the cortex of the BAI, LABI and LABWI-30 groups (Figure. 4D upper and Figure. 4E). Notably, staining for the excitatory neuronal marker neurogranin (NRGN) revealed decreased cell density in the cortex of the BAI group, but preserved cell density in the other groups (Figure. 4D lower and Figure. 4F). We next assessed whether the glial cells maintained their structural properties after NMP. Staining for microglial marker (IBA1) produced fragmented signals with signs of cellular destruction in the CA1 field of all the perfused brains, but preserved density in the dentate gyrus of BAI, LABI and LABWI-30 groups (Figure. 4, G to I). In contrast, staining for astrocytic marker (GFAP) revealed fragmented signals only in the LABWI-60 brains and preserved astrocyte density in other groups (Figure. 4, J to L). To dissect the potential mechanisms, immunohistochemisty analysis for the hypoxia-induced markers (HIF-1α, HSP70 and NRF2) was conducted. Staining of these markers in the cortex demonstrated that the BAI brains suffered obvious ischemic injuries compared to the normal controls (Figure. S7). Collectively, with the supports of a functioning liver, the ischemic injuries were reduced.

3.6 Regulation of perfusate metabome profile by the liver in the NMP circuit

The metabolism function of the liver is considered as a prerequisite for normal brain function[34]. The Ultra High Performance Liquid Chromatography coupled to triple-quadrupole

Mass Spectrometry (UHPLC-QqQ-MS) metabolomics analysis documented different metabolome profiles between the BAI and LABI groups (Figure. S8, A and B). Glycine, serine and threonine metabolism was the most significantly different metabolic pathway, followed by methane metabolism, alanine, aspartate and glutamate metabolism, as well as arginine and proline metabolism (Figure. S8C). The heatmap of hierarchical clustering analysis showed the identified differentially expressed metabolites (screened by variable importance in the projection > 1 and $P < 0.05$) (Figure. 4M). The level of two inhibitory neurotransmitters (γ-Aminobutyric acid and Glycine) increased, but the level of an excitatory neurotransmitter (L-Glutamic acid) decreased, during NMP in the BAI versus LABI brains (Figure. 4N). In addition, the level of two aromatic amino acids (L-Phenylalanine and L-Tryptophan) elevated in the BAI group, but with no significant difference in the level of detected branched chain amino acids between the two groups (Figure. 4N). These findings are in consistence with well-clarified roles of neurotransmitters and aromatic amino acids in the pathogenesis of hepatic encephalopathy [27]. Interestingly, the roles of 26 out of 39 identified differentially expressed metabolites in brain function have not been reported in the literature. The above results suggest the crucial role of liver metabolic function in brain resuscitation.

3.7 Different gene expression profiles in the LABI versus BAI brains

By comparing global gene expression profiles using a whole genome gene array approach, we identified a total of 129 differentially expressed genes (DEGs) (up-regulation, 107 genes; down-regulation, 22 genes) in the cortex of brains after 6-hour NMP in LABI versus BAI groups with an altered expression level of more than 2-fold at a statistical significance level of $P < 0.01$ (Figure. 5A). The DEGs could be divided into 5 major groups, including *regulation of synapse and axon* (15 DEGs), *regulation of neurotransmitters* (9 DEGs), *neural system process and development* (42 DEGs), *sensory perception* (20 DEGs) and *wound healing* (20 DEGs), suggesting that the liver directly affected the neural signal transduction, which is in accordance with the EEG results. In the *regulation of synapse and axon* group, a subgroup of genes, including *GPER1*, *PENK*, *FAM196A*, *GRIP2*, *ADORA2A*, *F2R*, *TAC1* and *NTRK2,* were involved in regulation of synaptic transmission (Figure. 5B). Addition of a liver in the perfusion circuit up-regulated the expression of this group of genes except *GRIP2* when compared to the BAI brains. Notably, *GPER1*, *GRIP2*, *ADORA2A*, *F2R* and *NTRK2* were also involved in

regulation of neurotransmitter (Figure. 5C). Besides, the expression of several other neurotransmitter-related genes (*RGS9*, *FGR*, *AGT* and *RORA*), were up-regulated in the LABI group. In terms of *neural system process and development*, the liver-assisting NMP up-regulated the expression of *NTS*, *NTN5*, *ARHGEF15*, *VCAM1*, *VIM*, *PPP1R1B* and *CRB2*, but down-regulated the expression of *FUT9*, *STRIP1* and *NEUROD6* (Figure. 5D). Most of these genes were related to the development of central nervous system. It is largely unknown that how these genes may participate in the process of consciousness. Interestingly, a large number of genes related to sensory perception of sight (*GPER1*, *ARHGEF15*, *NTRK2*, *RGS9*, *FGR*, *NTS*, *VIM*, *GNG11*, *GNG4*, *COL18A1* and *GPR88*), pain (*ADORA2A*, *F2R*, *TAC1* and *LXN*), taste (*TCF7*, *GNG11* and *GNG4*), sound (*USP53*), smell (*GNAL*) and heat (*LXN*) were differentially expressed between the BAI and LABI groups (Figure. 5E). The majority of these genes except *GNG4* and *LXN* were up-regulated in the LABI brains, suggesting enhanced sensory perception in this group. Finally, a number of genes related to *wound healing* were up-regulated in the LABI groups (Figure. 5F), indicating that the liver provides additional protection for the brains suffering from ischemia.

3.8 Distinct proteomics profiles in the LABI versus BAI brains

We further explored the molecular mechanism underling the protective effects of a functioning liver on the brain by proteomics analysis. To visualize the protein expression differences, we applied unsupervised hierarchical clustering analysis (HCA) on the significant proteins with mean-centered label-free quantification (LFQ) intensity transformed with $\log_2$ function (Figure. 5H). A total of 44 differentially expressed proteins were identified in the cortex of brains in the LABI versus BAI groups. Notably, we observed a high percentage (18/33, 43.2%) of annotated proteins (GPS1, MCCC2, DNM2, GRM5, CADPS2, SLC6A11, KCNMA1, CNTNAP2, KCNAB2, KCNA2, REEP1, GUD1, CUTA, GAD1, GNAZ, hint1, Cldn11 and ACTR10) related to *regulation of synapse and axon*. In brain, glutamate and GABA are two major neurotransmitters, which play excitatory and inhibitory functions, respectively. Addition of a liver in the NMP circuit increased expression of two glutamate receptors (GLUD1 and GRM5), but decreased expression of one GABA receptor (SLC6A11) and glutamate decarboxylase 1 (GAD1, decarboxylating glutamate into GABA), which suggests stronger excitatory but weaker inhibitory neuronal signaling in the cortex of LABI versus BAI group.

Interestingly, reduced protein expression of one calcium-activated potassium channel (KCNMA1), two voltage-gated potassium channel (KCNA2 and KCNAB2), and a cell adhesion protein (CNTNAP2) (functioning in the localization of voltage-gated potassium channel complex), were found in the LABI versus BAI cortex. Studies have showed that these potassium channels are crucial for the action potential repolarization and neurotransmitter release[35-38]. Reduced activity leads to an increase in postsynaptic excitatory responses. Collectively, the proteomics analysis showed a clear enhanced excitatory neural signaling in the LABI versus BAI cortex.

4. Discussion

The liver-assisting brain NMP model is established based on clinical practice. First of all, to simulate controlled donation after circulatory death[6], exsanguination and ventricular injection of potassium chloride was used to induce cardiac arrest and the brain was harvested after 5-min no-touch time. Meanwhile, it has been showed that the core temperature largely affects the brain resuscitation[32]. The study reported full neurological recovery from profound (18.0°C) acute accidental hypothermia by active invasive rewarming technique. In the study reported by Vrselja et al, the brains were preserved on ice for three hours after 1-hour warm ischemia[16]. Besides, the Hemopure-based perfusate used did not contain any immune cells, which role out the profound effects of immune response in ischemia-perfusion injuries[16]. Therefore, their results might over-estimate the brain tolerance to "prolonged" (4-hour) ischemia. In the current study, to represent the majority of clinical conditions, the brains only suffered normothermic ischemia before NMP and the perfusate was a whole blood cell-based one. Therefore, the model might better simulate the clinical conditions when compared with the previously reported models[16,25,26].

To our knowledge, the standard method to assess consciousness *ex vivo* has not been reported. In the early studies and the recent report[16,17,39], EEG was used to detect the signs of consciousness. However, the EEG activity itself would not reliably signal a conscious brain since such activity is always detected in people who are under general anaesthesia[40]. In this study, instead of isolating the brains from the skull, we preserved the brains in the skull and disconnected the head from the body between C7 and T1 vertebra, which makes it feasible for testing brainstem reflexes, ability to breathe, and particularly response to external stimuli. Therefore, we can use the FOUR score, a clinical scoring system to assess the state of consciousness[23]. The results suggested a almost fully conscious state in some experiments, although the FOUR score could not achieve its maximum of 16 score, due to the disability of language communication and incomplete respiration movement without the chest. The EEG changes under sound and light stimulus further supports the awake state of the perfused brains. These direct evidence show that consciousness can be restored and maintained *ex vivo*.

One of the important findings in this study is the critical role of a liver in the *ex vivo*

restoration of consciousness. This finding is in consistent with the presence of severe coma in patients suffering primary graft non-function post-liver transplantation, which requires an urgent re-transplant for life-saving[41]. We found that addition of a liver in the NMP circuit can reduce the levels of inhibitory neurotransmitters and aromatic amino acids in the perfusate, which is consistent with clinical observations in hepatic encephalopathy[27]. Moreover, the RNA sequence analysis showed that the liver-assisting NMP enhanced the expression of a number of genes related to synapse formation and function, neurotransmitter, and sensory perception. The proteomics analysis demonstrated that the majority of differentially expressed proteins were involved in regulation of synapse activity and the excitatory neural signaling was stronger in the LABI versus BAI groups.

Ex vivo maintenance of consciousness would raise important ethical consideration. In this study, the pig brains were dissected under full anesthesia and procured after cardiac arrest. The perfusions were discontinued after 6-hour NMP, although our preliminary result showed that the consciousness can be maintained for more than 22 hours. Painkiller was used during *ex vivo* brain NMP and no obvious sufferings (if we can interpret them correctly) was recorded in any experiment. However, a standard ethical guideline should be outlined by the corresponding stakeholders according the international regulations. Most importantly, any attempt to use this technology in resuscitating human brain *ex vivo* should be forbidden before the corresponding international regulations or laws are approved.

Undoubtedly, there are a number of limitations in this study. Firstly, we tried to use pigs for food production instead of experimental animals. However, our institutional ethic committee only considered ethical application using experimental animals and the lab did not allow to conduct studies using animals for food production. Secondary, we did not document a full FOUR score in any experiment because it is almost impossible to get full score in an isolated head or brain according the criteria. It is suggested that EEG activity with responsiveness to transcranial magnetic stimulation (TMS) might be an alternative to assess consciousness in this circumstance. Finally, we showed that the liver-assisting NMP was able to regulate the metabome profiles of perfusate, enhance gene and protein expression related to synapse and neurotransmitter, and ameliorate ischemic injuries. However, the detailed molecular mechanism is still unclear due to the complexity of brain function and study design

of big animal experiments.

In conclusion, we report that *ex vivo* liver-assisting brain NMP can restore brain consciousness after "circulatory death" in pigs. Without use of any central nervous system stimulant, the maximum WIT after which the brain consciousness can be restored is about 50 minutes. After further development and optimization of the technology, the complete ischemia time that the brain can endure might be prolonged. The knowledge from this and following studies will probably help improve the technology of brain resuscitation, and update the current diagnostic criteria of death.

Acknowledgements

Funding

This work was supported by grants as follows: the National Natural Science Foundation of China (81970564, 81471583 and 81570587), the Guangdong Provincial Key Laboratory Construction Projection on Organ Donation and Transplant Immunology (2013A061401007 and 2017B030314018), Guangdong Provincial Natural Science Funds for Major Basic Science Culture Project (2015A030308010), Guangdong Provincial Natural Science Funds for Distinguished Young Scholars (2015A030306025), Special Support Program for Training High Level Talents in Guangdong Province (2015TQ01R168), Pearl River Nova Program of Guangzhou (201506010014), and Science and Technology Program of Guangzhou (201704020150).

Competing interests: None declared.

Data and materials availability: All data needed to evaluate the conclusions in the paper are present in the paper or the supporting information.

References:

1. Fernandez-Mondejar E, Fuset-Cabanes MP, Grau-Carmona T, Lopez-Sanchez M, Penuelas O, Perez-Vela JL *et al*. The use of ECMO in ICU. Recommendations of the Spanish Society of Critical Care Medicine and Coronary Units. *Med Intensiva* 2019; 43(2): 108-120.
2. Borjigin J, Lee U, Liu T, Pal D, Huff S, Klarr D *et al*. Surge of neurophysiological coherence and connectivity in the dying brain. *Proc Natl Acad Sci U S A* 2013; 110(35): 14432-14437.
3. COLE SL, CORDAY E. Four-minute limit for cardiac resuscitation. *J Am Med Assoc* 1956; 161(15): 1454-1458.
4. GRENELL RG. Central nervous system resistance; the effects of temporary arrest of cerebral circulation for periods of two to ten minutes. *J Neuropathol Exp Neurol* 1946; 5: 131-154.
5. Torke AM, Bledsoe P, Wocial LD, Bosslet GT, Helft PR. CEASE: a guide for clinicians on how to stop resuscitation efforts. *Ann Am Thorac Soc* 2015; 12(3): 440-445.
6. McGee A, Gardiner D, Murphy P. Determination of death in donation after circulatory death: an ethical propriety. *Curr Opin Organ Transplant* 2018; 23(1): 114-119.
7. Shapey IM, Summers A, Augustine T, van Dellen D. Systematic review to assess the possibility of return of cerebral and cardiac activity after normothermic regional perfusion for donors after circulatory death. *Br J Surg* 2019; 106(3): 174-180.
8. Hossmann KA, Zimmermann V. Resuscitation of the monkey brain after 1 h complete ischemia. I. Physiological and morphological observations. *Brain Res* 1974; 81(1): 59-74.
9. Zimmermann V, Hossmann KA. Resuscitation of the monkey brain after one hour's complete ischemia. II. Brain water and electrolytes. *Brain Res* 1975; 85(1): 1-11.
10. Kleihues P, Hossmann KA, Pegg AE, Kobayashi K, Zimmermann V. Resuscitation of the monkey brain after one hour complete ischemia. III. Indications of metabolic recovery. *Brain Res* 1975; 95(1): 61-73.
11. Hossmann KA, Sato K. Recovery of neuronal function after prolonged cerebral ischemia. *Science* 1970; 168(3929): 375-376.
12. Allen BS, Ko Y, Buckberg GD, Tan Z. Studies of isolated global brain ischaemia: II. Controlled reperfusion provides complete neurologic recovery following 30 min of warm ischaemia - the importance of perfusion pressure. *Eur J Cardiothorac Surg* 2012; 41(5): 1147-1154.
13. Verwer RW, Hermens WT, Dijkhuizen P, ter Brake O, Baker RE, Salehi A *et al*. Cells in human postmortem brain tissue slices remain alive for several weeks in culture. *Faseb J* 2002; 16(1): 54-60.
14. Onorati M, Li Z, Liu F, Sousa A, Nakagawa N, Li M *et al*. Zika Virus Disrupts Phospho-TBK1 Localization and Mitosis in Human Neuroepithelial Stem Cells and Radial Glia. *Cell Rep* 2016; 16(10): 2576-2592.
15. Barksdale KA, Perez-Costas E, Gandy JC, Melendez-Ferro M, Roberts RC, Bijur GN. Mitochondrial viability in mouse and human postmortem brain. *Faseb J* 2010; 24(9): 3590-3599.
16. Vrselja Z, Daniele SG, Silbereis J, Talpo F, Morozov YM, Sousa A *et al*. Restoration of brain circulation and cellular functions hours post-mortem. *Nature* 2019; 568(7752): 336-343.
17. White RJ, Albin MS, Verdura J. Preservation of viability in the isolated monkey brain utilizing a mechanical extracorporeal circulation. *Nature* 1964; 202: 1082-1083.
18. Warnecke G, Moradiellos J, Tudorache I, Kuhn C, Avsar M, Wiegmann B *et al*. Normothermic perfusion of donor lungs for preservation and assessment with the Organ Care System Lung before bilateral transplantation: a pilot study of 12 patients. *Lancet* 2012; 380(9856): 1851-1858.
19. Dhital KK, Iyer A, Connellan M, Chew HC, Gao L, Doyle A *et al*. Adult heart transplantation with

distant procurement and ex-vivo preservation of donor hearts after circulatory death: a case series. *Lancet* 2015; 385(9987): 2585-2591.
20. Nasralla D, Coussios CC, Mergental H, Akhtar MZ, Butler AJ, Ceresa C *et al*. A randomized trial of normothermic preservation in liver transplantation. *Nature* 2018; 557(7703): 50-56.
21. Hosgood SA, Saeb-Parsy K, Hamed MO, Nicholson ML. Successful Transplantation of Human Kidneys Deemed Untransplantable but Resuscitated by Ex Vivo Normothermic Machine Perfusion. *Am J Transplant* 2016; 16(11): 3282-3285.
22. Cai Y, Weng K, Guo Y, Peng J, Zhu ZJ. An integrated targeted metabolomic platform for high-throughput metabolite profiling and automated data processing. *Metabolomics* 2015; 11(6): 1575-1586.
23. Wijdicks EF, Bamlet WR, Maramattom BV, Manno EM, McClelland RL. Validation of a new coma scale: The FOUR score. *Ann Neurol* 2005; 58(4): 585-593.
24. Lam TI, Brennan-Minnella AM, Won SJ, Shen Y, Hefner C, Shi Y *et al*. Intracellular pH reduction prevents excitotoxic and ischemic neuronal death by inhibiting NADPH oxidase. *Proc Natl Acad Sci U S A* 2013; 110(46): E4362-E4368.
25. Jang C, Hui S, Zeng X, Cowan AJ, Wang L, Chen L *et al*. Metabolite Exchange between Mammalian Organs Quantified in Pigs. *Cell Metab* 2019; 30(3): 594-606.
26. Allen BS, Ko Y, Buckberg GD, Tan Z. Studies of isolated global brain ischaemia: III. Influence of pulsatile flow during cerebral perfusion and its link to consistent full neurological recovery with controlled reperfusion following 30 min of global brain ischaemia. *Eur J Cardiothorac Surg* 2012; 41(5): 1155-1163.
27. Prakash R, Mullen KD. Mechanisms, diagnosis and management of hepatic encephalopathy. *Nat Rev Gastroenterol Hepatol* 2010; 7(9): 515-525.
28. Mergental H, Perera MT, Laing RW, Muiesan P, Isaac JR, Smith A *et al*. Transplantation of Declined Liver Allografts Following Normothermic Ex-Situ Evaluation. *Am J Transplant* 2016; 16(11): 3235-3245.
29. Koch C, Massimini M, Boly M, Tononi G. Neural correlates of consciousness: progress and problems. *Nat Rev Neurosci* 2016; 17(5): 307-321.
30. Mashour GA, Hudetz AG. Neural Correlates of Unconsciousness in Large-Scale Brain Networks. *Trends Neurosci* 2018; 41(3): 150-160.
31. Michetti F, D'Ambrosi N, Toesca A, Puglisi MA, Serrano A, Marchese E *et al*. The S100B story: from biomarker to active factor in neural injury. *J Neurochem* 2019; 148(2): 168-187.
32. Hughes A, Riou P, Day C. Full neurological recovery from profound (18.0 degrees C) acute accidental hypothermia: successful resuscitation using active invasive rewarming techniques. *Emerg Med J* 2007; 24(7): 511-512.
33. Horn M, Schlote W. Delayed neuronal death and delayed neuronal recovery in the human brain following global ischemia. *Acta Neuropathol* 85(1): 79-87.
34. Felipo V. Hepatic encephalopathy: effects of liver failure on brain function. *Nat Rev Neurosci* 2013; 14(12): 851-858.
35. Contet C, Goulding SP, Kuljis DA, Barth AL. BK Channels in the Central Nervous System. *Int Rev Neurobiol* 2016; 128: 281-342.
36. Saint-Martin M, Joubert B, Pellier-Monnin V, Pascual O, Noraz N, Honnorat J. Contactin-associated protein-like 2, a protein of the neurexin family involved in several human diseases. *Eur J Neurosci* 2018; 48(3): 1906-1923.
37. Perkowski JJ, Murphy GG. Deletion of the mouse homolog of KCNAB2, a gene linked to

monosomy 1p36, results in associative memory impairments and amygdala hyperexcitability. *J Neurosci* 2011; 31(1): 46-54.
38. Lambe EK, Aghajanian GK. The role of Kv1.2-containing potassium channels in serotonin-induced glutamate release from thalamocortical terminals in rat frontal cortex. *J Neurosci* 2001; 21(24): 9955-9963.
39. Hirsch H, Tesch P. Recovery of the electrocorticogram of canine brains after complete cerebral ischaemia at 37 degrees and 32 degrees C. *Neurosurg Rev* 1982; 5(2): 49-54.
40. Brown EN, Lydic R, Schiff ND. General anesthesia, sleep, and coma. *N Engl J Med* 2010; 363(27): 2638-2650.
41. Chen XB, Xu MQ. Primary graft dysfunction after liver transplantation. *Hepatobiliary Pancreat Dis Int* 2014; 13(2): 125-137.

Figures

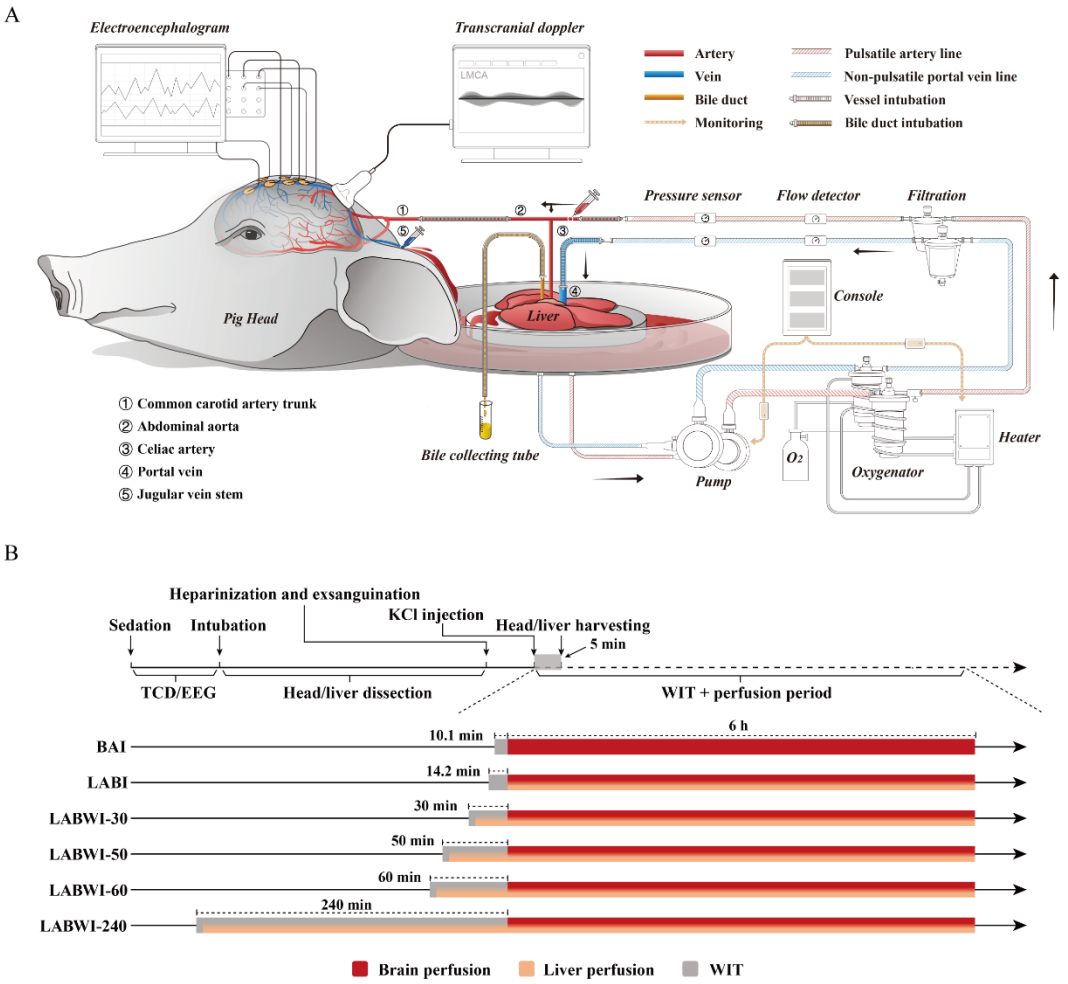

Figure. 1 The *ex vivo* brain normothermic machine perfusion (NMP) system and experimental workflow.

(A) Simplified schematic of the open-circuit perfusion system. The porcine head was connected to the perfusion system via a pulsatile artery line. In addition, the liver was connected to the system through a common artery line and a non-pulsatile portal vein line. Ports for arterial and venous sampling are shown. In this system, electroencephalogram (EEG) was performed to detect the electrical activity in the brain. The left middle cerebral arterial flow were detected by transcranial doppler (TCD). (B) Schematic depicting the experimental workflow and conditions. WIT, warm ischaemia time; BAI, brain alone immediately NMP; LABI, liver-assisting brain immediately NMP; LABWI-30, liver-assisting brain 30 min-WIT NMP; LABWI-50, liver-assisting brain 50 min-WIT NMP; LABWI-60, liver-assisting brain 60 min-WIT NMP; LABWI-240, liver-assisting brain 240min-WIT NMP.

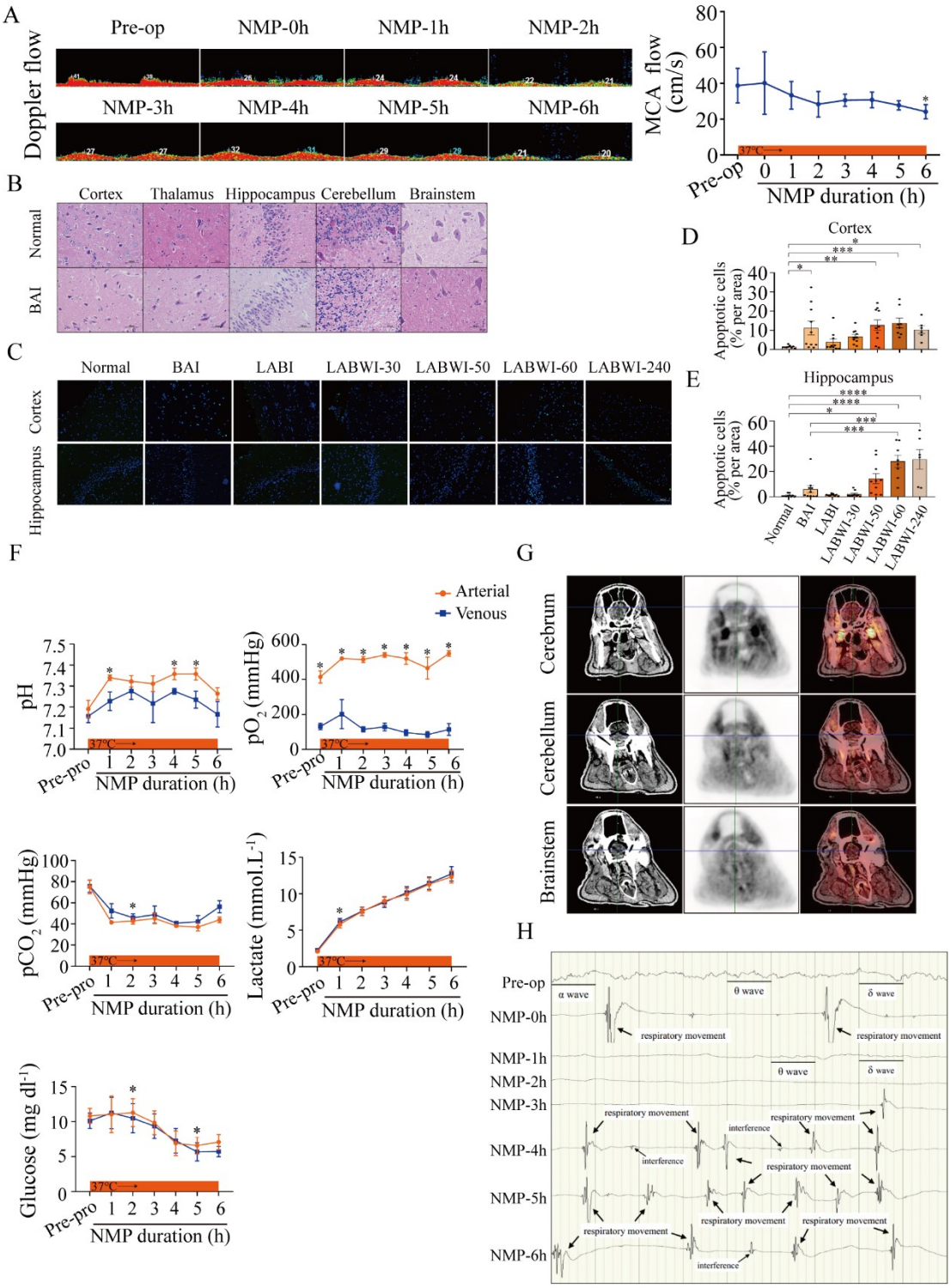

Figure. 2 *Ex vivo* normothermic machine perfusion (NMP) of brain alone can maintain vascular circulation, tissue integrity and metabolic activity.

(A) The transcranial doppler (TCD) demonstrating restoration of the middle cerebral arterial (MCA) flow by the *ex vivo* perfusion system in a representative brain. Mean ± s.e.m for statistics. Two-tailed paired t-test for each point. (B) Hematoxylin and eosin (HE) staining

(400×) of the cortex, thalamus, hippocampus, cerebellum, and brainstem after 6-hour NMP. (C) The terminal deoxynucleotidyl transferase-mediated biotinylated UTP nick end labeling (TUNEL) (200×) demonstrating apoptotic cells (green). (D) and (E) Histograms displaying normalized percentage of TUNEL positive nuclei in the cortex and hippocampus. Two areas (200×) of each brain for counting. (F) Paired measurements of arterial and venous samples indicating the arteriovenous gradients from the *ex vivo* brain NMP system. Mean ± s.e.m for statistics. Two-tailed paired t-test for each point. (G) The positron emission computed tomography (PET-CT) scan showing active glucose metabolism of the whole brain. (H) The electroencephalogram (EEG) testing results showing respiration movement but no organized lobal electrical activity. *Indicates a significant difference.

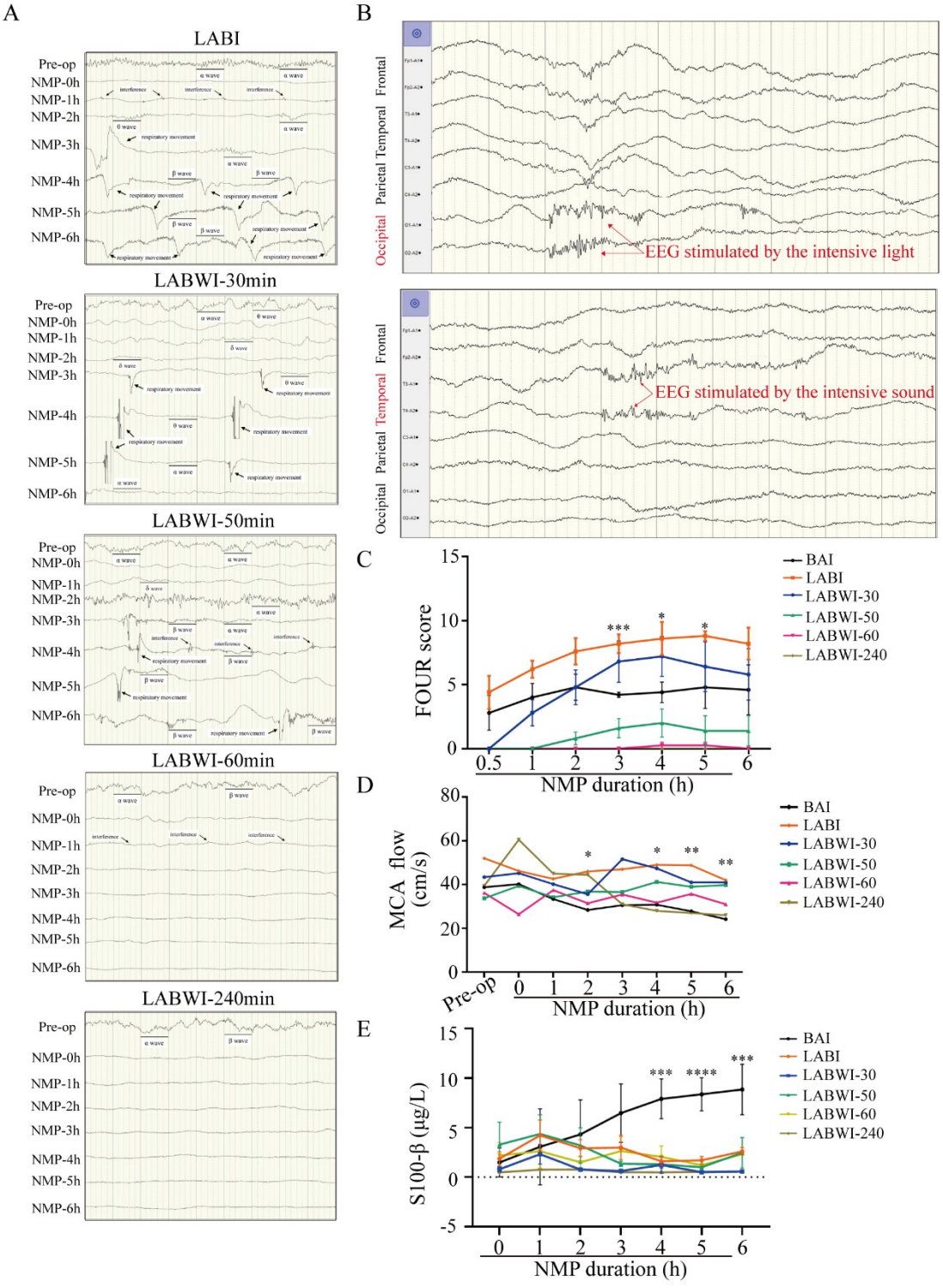

Figure. 3 A functioning liver is required for *ex vivo* restoration of brain consciousness.

(A) The electroencephalogram (EEG) testing results showing distinct conscious state of the five groups. (B) The EEG results demonstrating responses of one brain suffering 50-min WIT to strong light (upper) and sound (lower) stimuli. (C) The Full Outline of UnResponsiveness (FOUR) score in the five groups (BAI *vs* LABI, t-test. 3h: $p<0.001$; 4h: $p=0.025$; 5h: $p=0.046$).

(D) The middle cerebral arterial (MCA) flow in the five groups (BAI *vs* LABI, t-test. 2h: p=0.031; 4h: p=0.041; 5h: p=0.005; 6h: p=0.003). (E) The levels of S100-β, a biomarker of brain injury in the five groups (BAI *vs* LABI, t-test. 4h: p<0.001; 5h: p<0.0001; 6h: p<0.001). *p<0.05, **p<0.01, ***p<0.001, ****p<0.0001.

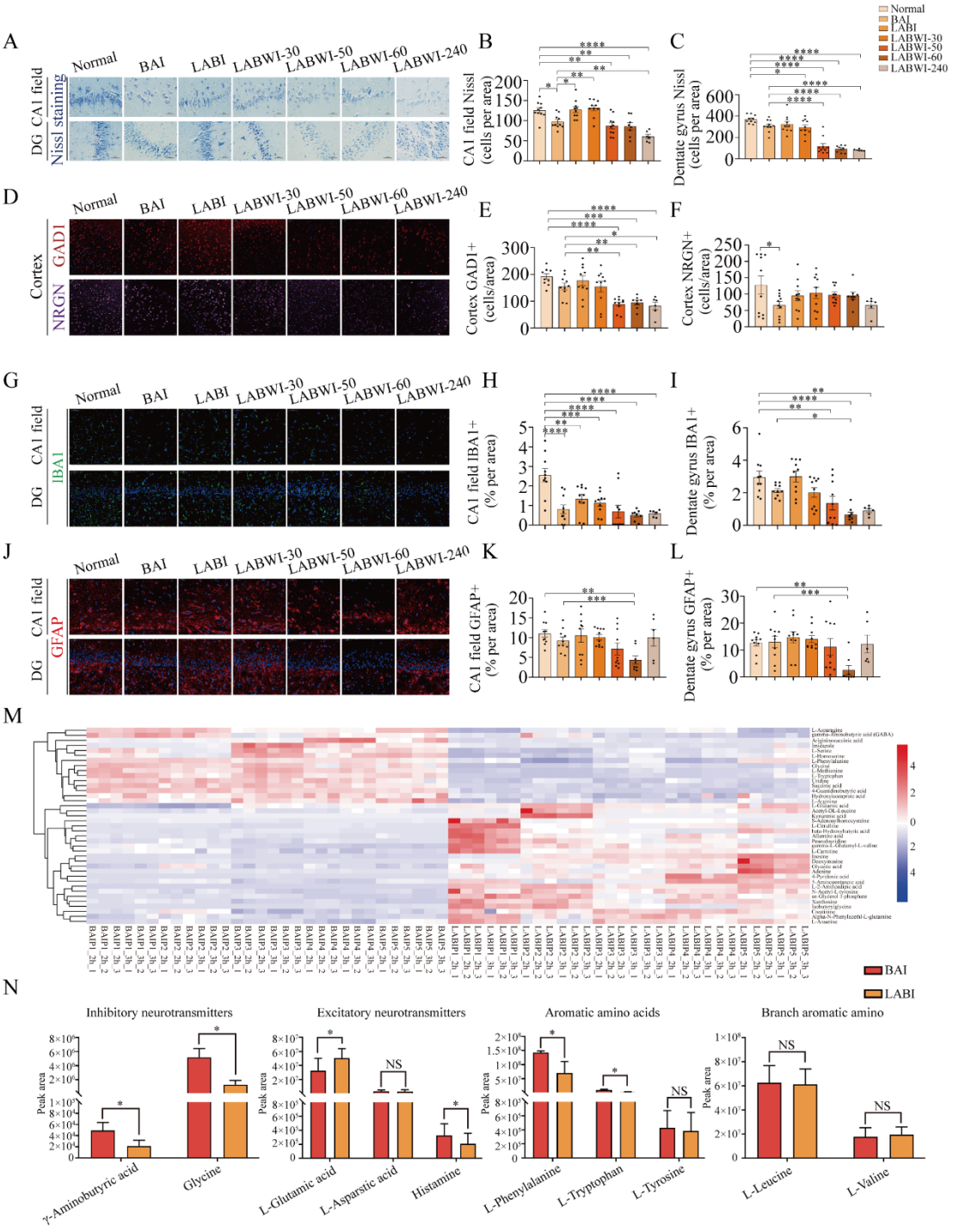

Figure. 4 The liver-assisting perfusion improves neuron viability and changes perfusate metabolome profiles.

(A) Nissl staining (400×) portraying soma and axon structure integrity of neurons in the hippocampus. Neurons with intact cell bodies were counted in the CA1 field (B) and dentate gyrus (C). Two areas (100×) of each brain were used for counting. Immunofluorescence staining for glutamate decarboxylase 1 (GAD1) (red) and Neurogranin (NRGN) (pink) of the

cortex (D). GAD1 (E) and NRGN (F) positive stained cells were counted. Immunofluorescence staining for ionized calcium binding adapter molecule 1 (IBA1) of the hippocampus (G). IBA1 positive stained cells were counted in CA1 field (H) and dentate gyrus (I). Immunofluorescence staining for glial fibrillary acidic protein (GFAP) of the hippocampus (J). Fluorescence area of GFAP was measured with ImageJ software in the CA1 field (K) and dentate gyrus (L). Two areas (200×) of each brain were used for counting. Heat map of the metabonomic differences in BAI versus LABI group, demonstrating 39 differentially expressed metabolites between the two groups (M). The color of each section is proportional to the significance of change of metabolites (red, up-regulated; green, down-regulated). The relative levels of inhibitory/excitatory neurotransmitters and aromatic/branched chain amino acids of the perfusate between the two groups (N). *p<0.05, **p<0.01, ***p<0.001, ****p<0.0001.

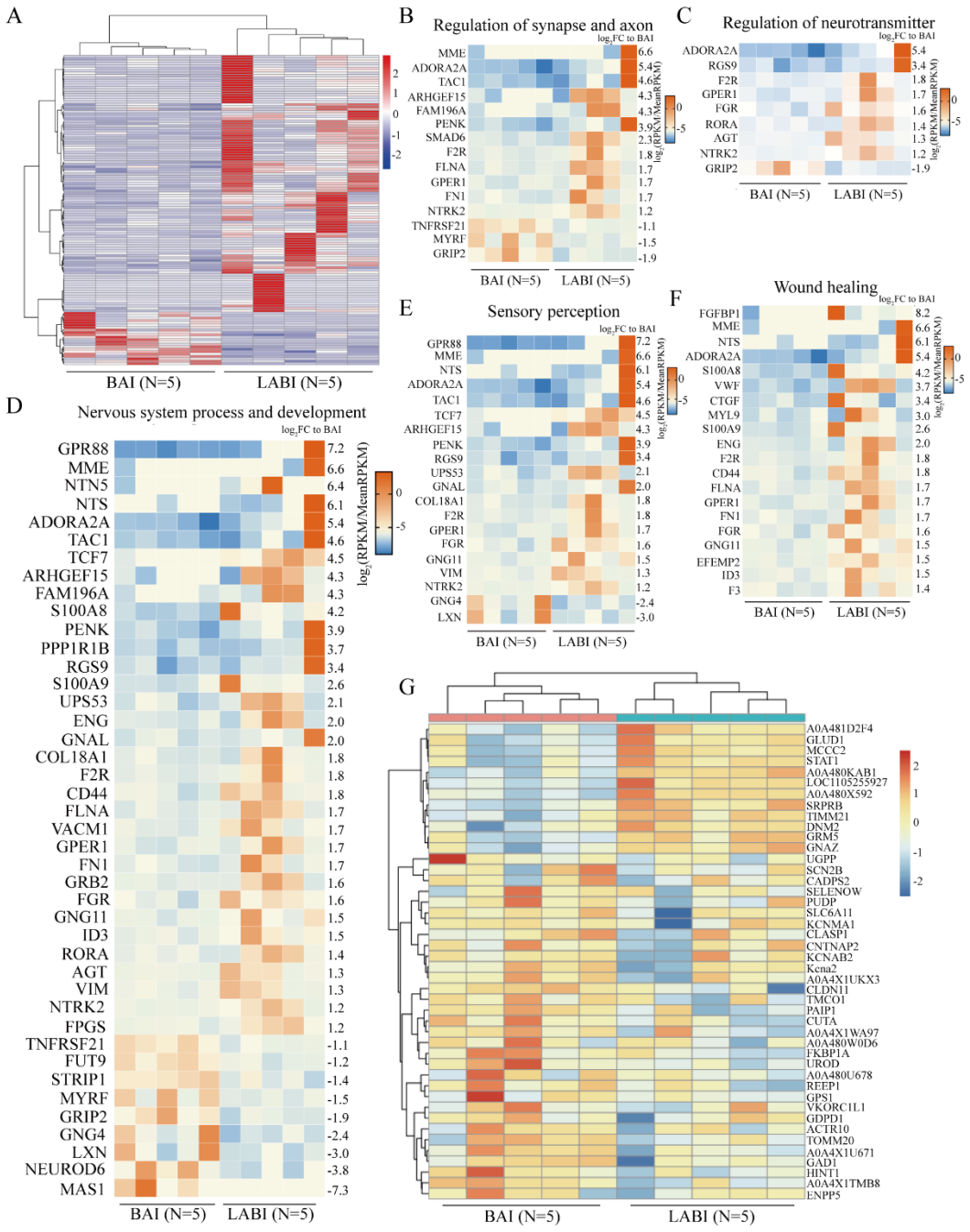

873

874 **Figure. 5 Differential expression of genes and proteins between the LABI and BAI groups.**

875 (A) The heat map showing the identified differentially expressed genes, containing 107 up-

876 regulated and 22 down-regulated genes in the LABI versus BAI cortex. The differentially

877 expressed genes enriched in *regulation of synapse and axon* (B), *regulation of*

878 *neurotransmitter* (C), *neural system process and development* (D), *sensory perception* (E) and

879 *wound healing* (F). The heat map showing the identified differentially expressed proteins in

880 the LABI and BAI cortex, including 12 up-regulated proteins and 32 down-regulated proteins

881 (G).